AUT Journal of Civil Engineering

AUT J. Civil Eng., 2(1) (2018) 11-28
DOI: 10.22060/ajce.2018.14235.5465

A Combined Model for Landslide Susceptibility, Hazard and Risk Assessment

R. Talaei*

Soil Conservation and Watershed Management Research Department, Ardabil Agricultural and Natural Resources Research and Education Center, Agricultural Research, Education and Extension Organization (AREEO), Ardabil, Iran

ABSTRACT: This paper proposes a combined model for landslide susceptibility, hazard and risk assessment based on a spatial prediction method and the fuzzy sets theory using geographical information systems (GIS). To evaluate landslide susceptibility and hazard in the study area in the northwest of Iran, the first step was the construction of a database, which includes three different data groups namely conditioning and triggering factors and the landslide inventory data. A landslide susceptibility model was constructed by using favorability function method and conditioning data including lithology, land use/land cover, elevation, slope aspect, slope gradient, slope curvature, distance to fault lines, distance to drainage network, distance to roads and distance to settlement. The selected landslides were of moderate to high intensity, which had occurred or reactivated at least once over the last 55 years. Landslide susceptibility map (LSM) transformed into landslide hazard map (LHM) by using the regional seismic and precipitation data, which are the two main factors in triggering landslides. Desirably, the accuracy of susceptibility and hazard models were determined 84.9% and 84.8%, respectively, by using the receiver operating characteristic (ROC) curve method. Layers of the landslide hazard potential (LHP) and resource damage potential (RDP), which characterized by landslide hazard levels and land use/land cover map of the area, were integrated based on the fuzzy algebraic product operator in order to determine the risk level due to landslides. Lastly yet most importantly, the results of the study integrated in the risk prevention and land use planning.

Review History:
Received: 19 March 2018
Revised: 18 May 2018
Accepted: 29 May 2018
Available Online: 13 June 2018

Keywords:
Damage
Hazard
Landslide
Prediction
Risk

1- Introduction

Landslides are globally widespread phenomena that frequently lead to loss of human life and property, as well as causing serious damage to natural resources [1-3]. Experts believe that about one quarter of the natural disasters in the world seems to be directly or indirectly related to landslides [4]. In Iran, landslides occur mostly along the two mountain ranges of Alborz and Zagros [5]; the annual direct loss caused by landslide has been estimated at 17 million dollars (in current value) [6]. The region in the south of Ardabil province in western part of Alborz mountain range and in the northwest of Iran has witnessed the occurrence of new landslides or re-activation of old ones annually [7]. Landslides cause significant damages to natural ecosystems and human-built-infrastructures in the south of Ardabil province.

Prior to this study done the region received very little attention by researchers. There were only a few landslide investigations to be found in earlier literature, but nothing of a comprehensive picture of any part of the region [8, 9]. In subsequent studies carried out in parts of the region, the causative factors in the landslide occurrence of the area is investigated and LSM was prepared using qualitative and quantitative methods. However, the fitness and accuracy of models have not been evaluated [10-13]. Presentation of any plan in order to mitigate losses and damage primarily requires landslide hazard and risk assessment in a region that is susceptible to landslides [14]. Landslide susceptibility, hazard and risk evaluation have become an essential tool in risk management as an integral part of land use planning and managing in disaster prone areas [15, 16].

Over the past 30 years, many papers related to the landslide susceptibility assessment (LSA) have been published [17, 18]. However, landslide hazard and risk evaluation are not a frequent topic in recent landslide literature [19, 20]. This might be due to the inherent difficulty of determining the landslide risk, lack of initiative and general models for risk assessment and multi-disciplinary nature of landslides risk analysis. Landslide risk can generally defined as "possible loss of life and property imposed by landslides that may occur to humans and their valuable objects" [21]. Landslides risk evaluation done in both basin scale [22-24] and site scale [25, 26]. The methods used to landslide risk assessment (LRA) can typically be labeled as being either a qualitative [27, 28] or quantitative procedures [29-31]. Apart from these two methods, semi-quantitative methods of LRA suggested based on fuzzy set theory as well [32]. A semi-quantitative landslide-risk assessment method, which would provide an evaluation of future landslide risks in a mountainous area in NW-Iran, was presented in this study. First step in every methods used in landslide hazard and risk assessment should

Corresponding author, E-mail: r.talaei@areeo.ac.ir

be the landslide susceptibility evaluation, which can be used to develop hazard map. Different methods used so far to evaluate the landslide susceptibility or hazard [33-37]. Although the algorithms for LSA, LHA and LRA are able to be defined entirely, they involve highly complex processes during the application stage [38-44]. Uncertainties in calculation of landslide susceptibility probability, transformation of landslide susceptibility rate to hazard prediction map and determination of vulnerability for resources at risk constitute the main limitations for landslide hazard and risk studies [45, 46]. In addition, the study area is a data-scarce region, and development of methods for landslide hazard and risk evaluation have always been a challenge in the region. However, there are very limitations in this study; the aim of the paper is to propose a combined model for landslide susceptibility, hazard and risk assessment, which makes it possible to zoom in on the high-risk areas. The present landslide susceptibility study is a unique endeavor in the region where favorability function analysis has been used for LSA and has been validate using receiver operating characteristic (ROC) curve analysis. High quality data and determination of suitable factors for landslide analysis of the region have crucial importance. Due to the difficulty in obtaining data sets and landslide inventory maps, the development of a combined new model for landslide susceptibility, hazard and risk assessment, including the use of statistical models and Fuzzy Set theory, have always been impeded in study region.

The main objectives of this study were: 1) to develop a landslide susceptibility assessment model for prediction zones prone to landsliding using favorability function, 2) to assess landslide hazard at the regional scale for the landslides with moderate and high intensity, which have occurred or reactivated at least once over the past 55 years in the region and 3) to semi-quantitative analysis of landslide risk for hazard scenario, assessing direct costs. For this purpose, landslide inventory map has been prepared in order to provide the data layer that is related to spatial and temporal landslide data. The probabilistic susceptibility model constructed by using the favorability function method and conditioning data. The susceptibility map transformed into landslide hazard model using triggering factors. The landslide susceptibility and hazard analysis results were validated using statistical methods: Receiver Operating Characteristics (ROC) method. Finally, the risk zonation map of landslide was prepared by using fuzzy algebraic product operator, based on two LHP and RDP maps.

2- Study Area

The study area is located in northwest of Iran and southern part of the Ardebil province (Figure 1). It covers an area of 1645.84 km^2. This area is one of the most exposed region to mass movements; while more than over 9.52% of area is potentially unstable [7, 13]. The study area subjected to many factors favoring the occurrence of landslides. About 175 landslides were mapped in the region covering 156 km^2. Landslides of the region classified as translational and rotational slides and combinations of the two, and landslide zones. Currently 103 cases of the landslides (58.9%) are active at the region. Interestingly, at least 60% of the studied landslides showed signs of activities over the last 55 years. Figure 2 shows parts of the study area affected by the landslides.

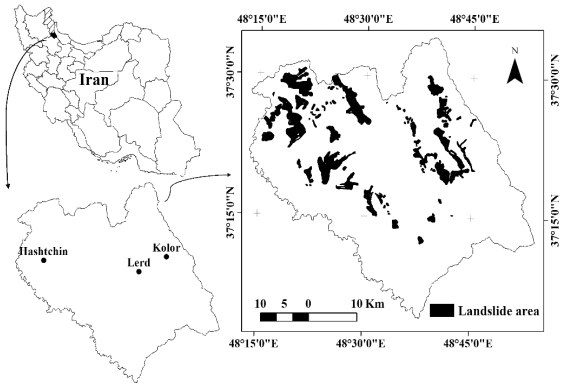

Figure 1. Location of the study area and spatial distribution of landslides [7]

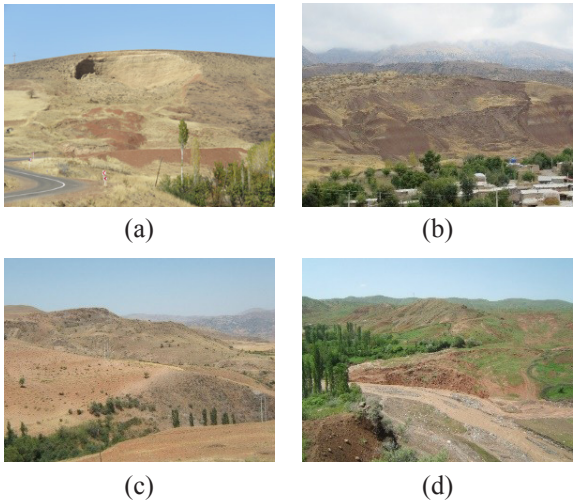

Figure 2. Field view of four landslides with in the study area [Author]: a) rotational landslides; b) translational-rotational combination; c) translational slide; d) earth flow

3- Methodology

The research methodology implemented into six phases: landslide inventory and data preparation, analysis of landslide causative factors, landslide susceptibility modelling, the data integration and preparation of landslide hazard map, the accuracy assessment of the models and landslide risk assessment. The methodological approaches shown schematically in Figure 3.

3- 1- Landslide inventory and input data preparation

Landslide inventory map is a preliminary step towards landslide susceptibility, hazard and risk assessment [47-49]. The present study began with the preparation of a detailed and reliable landslide inventory map based on interpretation of aerial photographs (scales: 1:20000 (1970), 1:40000 (2005) and 1:55000 (1957), by National Cartographic Center and National Geography Organization of Iran), field surveys, historical documents, and archived data for 1995 through 2016 years. The landslide inventory map was used to produce

the dependent variable, which was coded as "1" or "0" to indicate the presence and absence of landslide, respectively. Spatial database preparation is the important point for the landslide probability estimation [50]. The identification and mapping of a pertinent set of factors related to landslide involve previous information of their main causes [51]. Causative factors of landslides in the past can be considered as the most important factors in landslide occurrence in the future [52], so in the next phase of the study, thematic data layers pertinent to conditioning and triggering factors were prepared (Figure 4).

3- 2- Conditioning factors

During the research, databases were prepared for geological map and field observations. The geological mapping data and landslide inventory data have been stored in Arc-GIS geo-database format and the results of field studies in MS-Excel and Spss-22 tables. After collecting geological data such as lithology and geological structure from field observation, a geology map was prepared at 1:25000 scale. This map contains detailed information about the study area itself including the spacial relationship that exists between rocks and structures. Lithology or rock type and geological structures are the two most important factors in landslide occurrences due to their impact on rocks and soil resistance and permeability [50, 53, 54]. The lithology and fault maps were obtained and compiled from the 1:25000-scale geological map. Generally, there are thirteen group of rock types. The classification of lithology is shown in Figure 4a. In addition, proximity to faults is known to be an effective factor in landslide occurrence. Major and minor fault lines have an indirect impact on landslide occurrence through increased permeability as the result of rock crushing and expansion of alteration zones. In the study area, the closer to the fault with a weak plane, the larger is the number of landslides. Fault line buffer map is prepared from the geological map (Figure 4b). The land cover/land use map was produced in detail because it has been recognized as one of important independent variables to be used in the landslide risk analysis [41]. Land use/land cover map used in this study was derived from topographic maps (1:25000 and 1:50000 scales, by National Cartographic Center and National Geography Organization of Iran) and satellite images of Landsat ETM+-2002 using a hybrid classification scheme. This map was revised and completed based on the observations made during the field works. The boundaries of 16 different types of land use/land cover were digitized (Figure 4c).

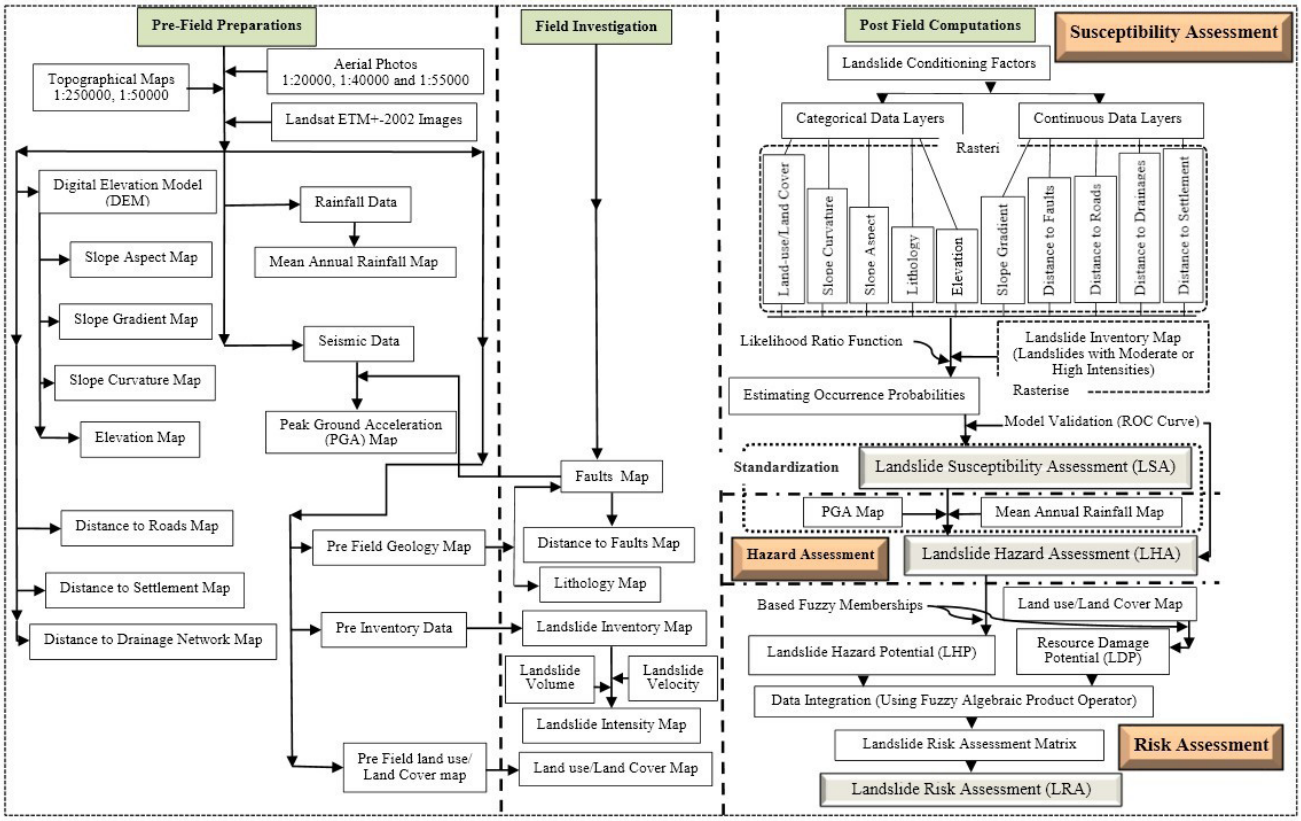

Figure 3. Flow chart showing source data and the methods used to landside susceptibility, hazard and risk assessment [Author]

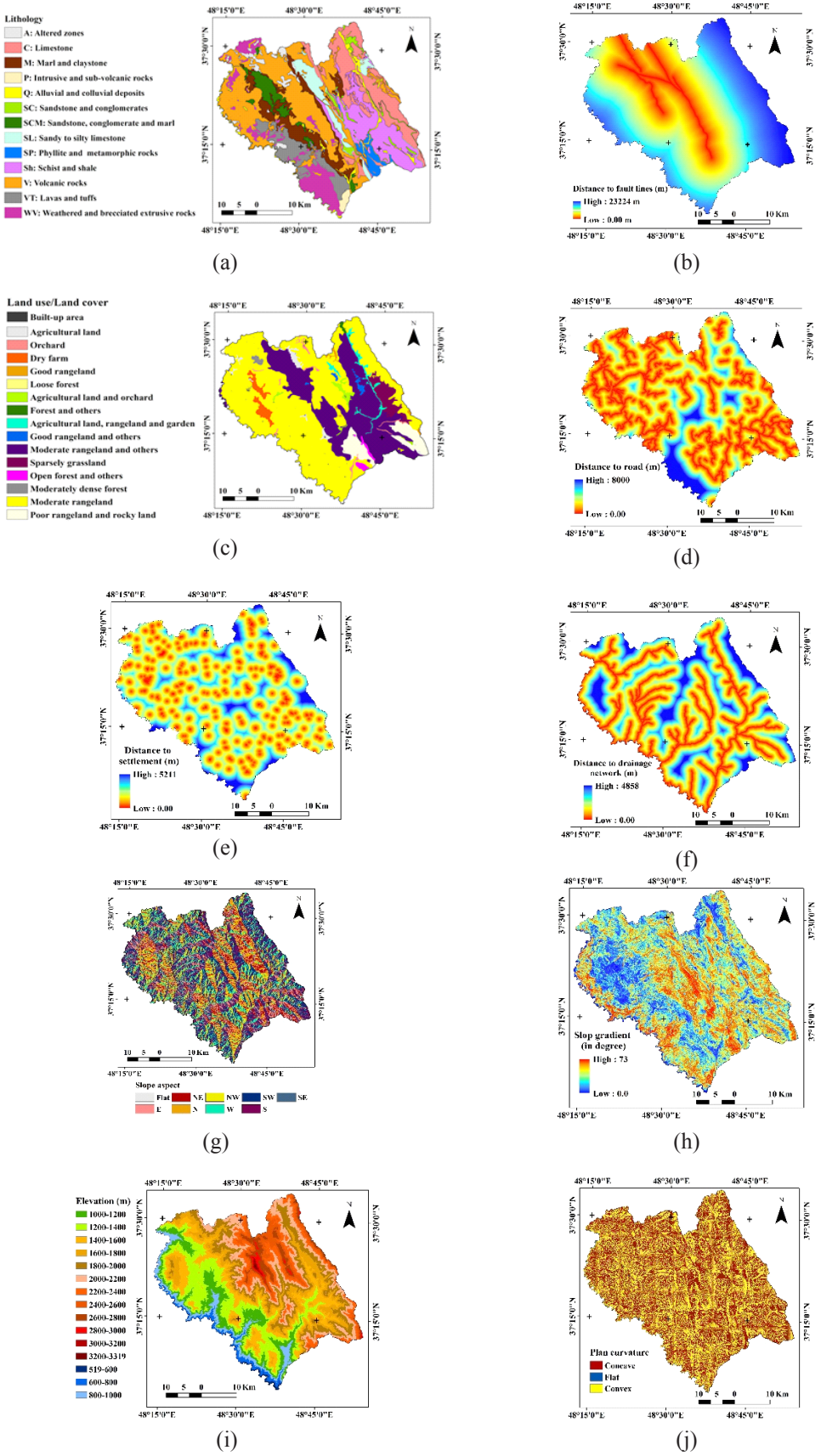

Figure 4. Landslide conditioning factor maps used for landslide susceptibility analysis [Author]: a) lithology; b) distance to fault lines; c) land-use/land cover; d) distance to roads; e) distance to settlement; f) distance to drainage network; g) slope aspect; h) slope gradient; i) elevation; j) slope curvature

Landslides may occur on the road and on the side of the slopes affected by roads. Landslide risk decreases as distance increases away from the road networks. Excavation, trenching, and other changes in slope due to road construction are usually sites of anthropologically induced slope instability [53, 55].

Similar to the effect of road construction, the excavation of slopes, mainly for house building, is an important destabilizing factor for the study area slopes. For this reason, the buffer areas are created on the path of the road as well as in villages and the cities to ascertain the effect of the roads and residential areas on the landslide occurrence (Figures 4d and e). Distance from drainage is another buffer raster, which introduces the influence of network of rivers (Figure 4f).

Slope angle and aspect have a great influence on the susceptibility of a slope to landsliding by controlling the amount and direction of runoff flow, vegetation density, soil temperature and moisture concentration [50, 53, 56]. A Digital Elevation Model (DEM) of the study area was prepared based on digital elevation contours with intervals of 20 m. Thematic data layers such as slope angle, slope aspect, elevation and slope curvature directly derived from the DEM. In this study, slope aspect was divided into nine classes: North (N), Northwest (NW), West (W), Southwest (SW), South (S), Southeast (SE), East (E), Northeast (NE) and Flat (Figure 4g). The elevations in the area range between 850 and 3324 m, and the slope angles range between 0° and 73° (Figure 4h). Relief data layer divided into fifteen classes of 200 m elevation (Figure 4i). The morphology represented by the slope curvature. The study area divided into three curvature groups: flat (straight (0)), concave (-1) and convex (+1) (Figure 4j).

3- 3- Triggering factors

In addition to the conditional factors, two triggering factors were also taken into account: seismicity and precipitation. Landslide triggering factors were used to transform the LSM to LHM [44, 46, 57, 58]. To this aim, precipitation and seismicity factors are examined (Figure 5). The rainfall effects on landslides occurrence of the region have been considered as the annual long-term mean precipitation map (based on historical rainfall data for area during the time period of 1986-2015). To determine the mean annual rainfall map-layer, the Equation 1 was used and the isohyet map at 1:25000 scale was prepared (Figure 5a) [59].

$$\text{Mean annual rainfall} = 471.162 - (X \times 4.81) + (Y \times 0.002) + (Z \times 0.063) \quad (1)$$

In this equation, X=longitude)degree(; Y=latitude)degree(and Z=elevation)meter above sea level).

Although the indirect impacts of minor and major faults on landslide occurrence are mainly through crushing and increased permeability of the surrounding rocks, penetration of hydrothermal liquid and expansion of the alteration zones; their direct impacts through seismic activity in the region should not be ignored or underestimated [60]. Seismic hazard describes natural phenomena caused by an earthquake that have the potential to cause harm such as induced landslide [61]. Landslides recorded in North and North-West of Iran following the Roodbar earthquake in 1990 is perhaps the best indicative of the effect of this phenomenon in occurrence of landslides in the study area [62, 63]. To simplify the induction of earthquake in landslide process, shear force is considered along a discontinuous rupture surface as the only unstable factor. For a quasi-static analysis, this force is assumed to be arisen from Peak Ground Acceleration (PGA) [64]. In order to represent hazard through a hazard map, it is necessary to reduce the hazard curve to a single value for each position. This is typically done by choosing the intensity value having a 10% chance of exceedance in 50 years [20, 65]. Taking into account the activity of landslides in the study area during the last 55 years, a scenario of future landslide occurrence has been adopted for the next 55 years, which compares to that verified in the past. Seismic hazard is quantified by two parameters: a level of hazard and its recurrence interval or frequency: for example, an earthquake with a recurrence interval of 500 years, and peak ground acceleration (PGA) with a return period of 475 years.

Seismic risk, on the other hand, describes a probability of occurrence of a specific level of seismic hazard or loss over a certain time (e.g., 50 years), and is quantified by three parameters: probability, a level of hazard or loss, and exposure time. For example, a 5 percent probability that an earthquake could be expected in 50 years in an area and a 10 percent probability that PGA could be exceeded in 50 years at a site are both seismic risk [66]. In order to evaluate the impact of the earthquake in landslide occurrence, a PGA map was reproduced corresponding to a return period of 475 years for 10% probability of exceedance over a 50-year return period. Based on the produced PGA map, the values obtained for study area range between 0.49 and 0.58 (g). The resulting map is shown in Figure 5b.

All data layers were transformed in raster format with pixel size of 50m×50m, therefore the area grid was 708456 rows by 12 columns with a total of 8501472 cells. This resolution was used for all subsequent processing and analysis for each landslide factor and the susceptibility, hazard and risk model. In implementing susceptibility model, 75% of the landslide pixels have been randomly selected to estimate the occurrence probabilities for future landslides and the 25% remaining pixels were retained for assessment of model accuracy by using ROC curve [42, 67, 68].

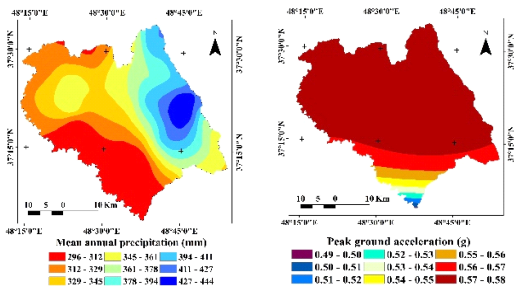

(a) (b)

Figure 5. Landslide triggering conditioning factor maps [Author]: a) annual long-term average precipitation density map and b) Peak Ground Acceleration (PGA) map of study area for a return period of 475 years

3- 4- Susceptibility assessment

A prediction model based on the likelihood ratio as the favorability function model were used to determine areas

likely to be affected by future landslides. To express this idea point c has been considered with m pixel values ($c_1,\ldots, c_i$) in the region [69, 70]. The study area was divided into two non-overlapping sub-areas: the portion including landslides M and the remaining areas without landslides $\bar{M}$. Considering that a pixel is from M and $\bar{M}$, the related multivariate frequency distribution can be depicted as $f\{c_1,\ldots,c_m/M\}$ and $f\{c_1,\ldots,c_m/\bar{M}\}$, respectively. The likelihood function, which is the ratio of two frequency distribution, can be defined at point c as [69, 71]:

$$\lambda(c_1,\ldots,c_m)=(f\{c_1,\ldots,c_m/M\})/(f\{c_1,\ldots,c_m/\bar{M}\}) \quad (2)$$

At pixel c the categorical and continuous data layers are separated and the first k layers and the remaining h layers represent categorical data layers and continuous data layers, respectively. The following formula $f\{x_1,\ldots,x_k, y_1,\ldots,y_h /M\}$ and $f\{x_1,\ldots,x_k, y_1,\ldots,y_h /\bar{M}\}$ denotes the multivariate frequency distribution functions and the k values, $x_1,\ldots,x_k$, and h values $y_1,\ldots..,y_h$ represent categorical data layers and continuous data layers, respectively. Then, the form of likelihood ratio functions denoted in Equation 2 will be as follow:

$$\lambda(x_1,\ldots,x_k,y_1,\ldots,y_h)=(f\{x_1,\ldots,x_k,y_1,\ldots,y_h/M\})/(f\{x_1,\ldots,x_k,y_1,\ldots,y_h/\bar{M}\}) \quad (3)$$

By considering an individual categorical layer with the distribution of occurrences of landslides, each of univariate likelihood ratio functions can be estimated:

$$\lambda(x:x_i)=(\text{number of landslide pixels in } x_i \text{ category of the ith layer})/(\text{number of non- landslide pixels in } x_i \text{ category of the ith layer}) \quad (4)$$

linear combination of independent variables [51, 72]. A In this study, discriminant analysis is used to estimate the likelihood ratio function for continuous data layers $\lambda(y_1,\ldots, y_h)$ for a pixel with h pixel values ($y_1,\ldots, y_h$). The simplest way to achieve this is through a discriminant function is a latent variable which is created as a linear combination of discriminating (independent) variables, such that;

$$D=a+b_1x_1+\ldots+b_px_p \quad (5)$$

where the b_1 through b_p are discriminant coefficients, the x_p are discriminating variables (predictors or conditioning factors), and a is a constant. In order to assess functionality of control in producing meaningful differences among target groups, the eigenvalues and Wilks' lambda tables are provided by discriminate analysis procedure to test how well the discriminant model fit the data as a whole. The values $\lambda(x_1,\ldots,x_k, y_1,\ldots, y_h)$ were calculated at each pixels employing the obtained functions:

$$\lambda(x_1,\ldots,x_k,y_1,\ldots,y_h)=\lambda(x_1,\ldots,x_k).\lambda(y_1,\ldots,y_h) \quad (6)$$

where $\lambda(x_1,\ldots, x_k)$ is an estimate of $\lambda(x_1,\ldots, x_k)$ and $\lambda(y_1,\ldots, y_h)$ is an estimate of $\lambda(y_1,\ldots, y_h)$. A range from 0 to ∞ shows the values of $\lambda(x_1,\ldots,x_k,y_1,\ldots,y_h)$ and the location most likely to be affected by future landslides are determined by the largest estimated values. The estimated value were normalized between a range of 0 to 1; 0 indicating no landslide susceptibility, and 1 indicating the highest susceptibility to landslides. The susceptibility values obtained in each pixel were converted to a raster map by using Arc-GIS software. The values of susceptibility were reclassified into five classes (very low, low, moderate, high, and very high) by standard deviation method.

3- 5- Hazard modelling

The procedure started with the development and evaluation of a probabilistic susceptibility model, which subsequently was transformed into a hazard map. Landslide models without landslide information like the return period and intensity (volume and speed of mass) of landslides cannot be correctly defined as hazard models [20, 51]. The inventory maps were used to collect temporal and spatial data on the landslides occurred in the region during the years 1960 through 2015. Velocity and volume of landslides have been determined based on landslide inventory map, and this information has been employed to estimate the landslides intensity in the region (Tables 1 and 2) [73-76]. Landslide velocity is often a proxy for landslide type and classified accordingly [77]. In large landslides, the excepted creep cases are considered of having, at least, moderate intensity [78]. The landslides with moderate and high intensity, which have occurred or reactivated at least once over the past 55 years in the region, were selected for landslide hazard analysis [7, 79]. The probabilistic susceptibility model was constructed by using the favorability function method and conditioning data including lithology, land use/land cover, elevation, slope aspect, slope gradient, slope curvature, distance to fault lines, distance to drainage network, distance to roads and distance to settlement. The probability of slope failure is calculated based on the data of the independent variables and landslide condition of the pixels using the favorability function method. The susceptibility map was transformed into landslide hazard model using triggering factors that include both seismic and precipitation data (Figure 6).

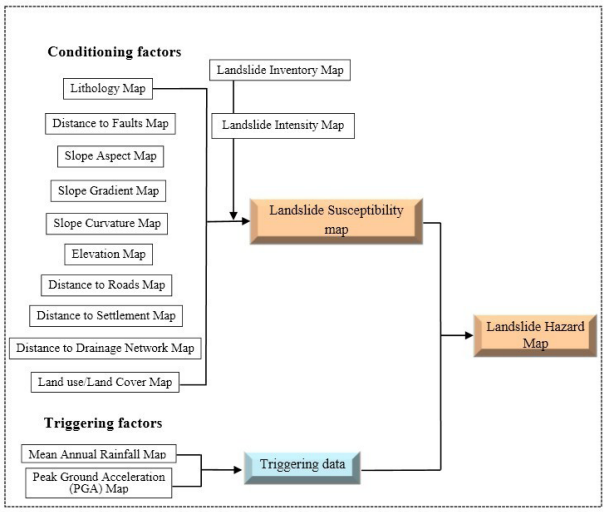

Figure 6. Flow diagram showing the method used to model landslide hazard in this study

Table 1. Single landslides intensity, in four classes, based on the estimated landslide volume and the expected landslide velocity [73-76, modified]

Estimated volume (m^3)	Description	Expected landslide velocity			
		Very rapid to rapid-moving flow	Rapid translational or translational-rotational slides	Slow translational or translational-rotational slides	Slow rotational slides
>5000 <50000	Small	Slight (1)			
> 50000 <250000	Medium	Medium (2)	Medium (2)	Slight (1)	Slight (1)
>250000 <1000000	Medium-large	High (3)	High (3)	Medium (2)	Medium (2)
>1000000 <5000000	Very large	Very high (4)	High (3)	High (3)	Medium (2)
>5000000	Extremely large	Very high (4)	Very high (4)	Very high(4)	High (3)

Table 2. Ranking of the intensity of landslide zones [73-76, modified]

Types of mass movement zones	Expected landslide velocity			
	Very slow	Slow	Rapid	Very rapid
Unmappable zones		Medium (2)	High (3)	Very high (4)
Widespread zones		Medium (2)	High (3)	Very high (4)
Creep zones	Slight (1)	Slight (1)		
Widespread and Creep zones		Medium (2)		

Transformation of LSM into a hazard model requires consideration of landslide triggering factors: mean annual precipitation map-layer and seismic data [44, 80, 81]. Next, for the creation of a landslide hazard map, the LSM and triggering factors were overlaid. For overlaying the LSM and the triggering factors, they must be standardized to a common dimensionless scale. The following Equation 7 is what should be used to implement a unity-based normalization [82]:

$$m(x_1,\ldots,x_k,y_1,\ldots,y_h)^{New}=(m(x_1,\ldots,x_k,y_1,\ldots,y_h)^{Old}-Min(m(x_1,\ldots,x_k,y_1,\ldots,y_h)))/(Max(m(x_1,\ldots,x_k,y_1,\ldots,y_h))-Min(m(x_1,\ldots,x_k,y_1,\ldots,y_h))) \quad (7)$$

where $X(^{Old})$ and $X(^{New})$ mean input and output data, $Min(X_i)$ and $Max(X_i)$ are the maximum and minimum of the input data, respectively. The $m(x_1,\ldots,x_k, y_1,\ldots, y_h)$New was used as favorability function in this study with a range from 0 to 1. The future location of probable landslides was estimated by the pixel with the largest calculated $m(x_1,\ldots,x_k, y_1,\ldots, y_h)$ New near 1. A predictive map showing the relative hazard level was produced for the area of study based on each pixels' computed values.

3- 6- Accuracy assessment

The accuracy of landslide susceptibility and hazard predictive models was calculated by drawing receiver operating characteristic (ROC) curves and by calculating the area under the ROC curve (AUC). A percentage of observations (pixels) with landslides, being predicted correctly by model, is called sensitivity (Equation 8) (Probability of correctly identifying a positive or the true positives).

$$Sensitivity=n_{tp}/(n_{tp}+n_{fn}) \quad (8)$$

n_{tp}: Number of true positive decisions; ntn: Number of false negative decisions

The specificity of the model has been shown based on the percentage of correct classified observations (pixels) with no landslides (Probability of correctly identifying a negative or true negatives) (Equation 9).

$$Specificity=n_{tn}/(n_{tn}+n_{fp}) \quad (9)$$

N_{tn}: Number of true negative decisions; N_{fp}: Number of false positive decisions

Commonly, ROC curve is plotted by using true positive rate (sensitivity) against false positive rate (1– specificity) for different cut-points of test, starting from coordinate (0, 0) and ending at coordinate (1, 1). False positive rate (1 – specificity) is represented by x-axis and true positive rate (sensitivity) is represented by y-axis. The area under the curve varies from 0 to 1. If the area under the curve is equal to 1 in a model, it will carry out the best and most complete prediction.

3- 7- Risk assessment

In recent years, development of approaches for LRA has always been a challenge. In the present study, a method for LRA, based on fuzzy set theory, has been developed and

implemented to generate LRA map for southern region of Ardabil province, NW-Iran. The fuzzy set theory has been proposed in 1965 by Zadeh [83]. The fuzzy logic theory is based on fuzzy sets which are a natural extension of the classical set theory. Unlike classical set theory, fuzzy set theory is flexible and focuses on the degree of being a number of a set. Membership value of elements are computed depending upon varying degrees of support on a phenomenon [32]. The membership function embodies the mathematical representation of membership in a set, and the notation used throughout this text for a fuzzy set is a set symbol with a tilde underscore, say A, where the functional mapping is given as:

$$\mu A(x) \in [0, 1] \quad (10)$$

Moreover, the symbol μA(x) is the degree of membership of element x in fuzzy set A. Therefore, μA(x) is a value on the unit interval that measures the degree to which element x belongs to fuzzy set A; equivalently, μA(x) = degree to which x ∈ A. The fuzzy membership values of different classes of the LHP and RDP were assigned based on a linguistic scale derived from recorded inventory data and expert knowledge. Exclusive rate values in hazard map prepared for the region is in accordance with the linguistic law (Table 3) [32]. In this region, the highest degree of membership fuzzy is given to buildings and roads and the lowest rates are given to forestlands (Table 4).

Table 3. Linguistic rules for risk scoring of landslide hazard levels [32, modified]

Fuzzy membership value for landslide hazard potential (LHP)	Linguistic rules for risk scoring	Landslide hazard zones
1	Landslides have occurred extensively and will occur frequently	Very high hazard
0.80	The evidence of landslide activity can be seen in most regions. Most of the probable landslides occur under adverse conditions.	High hazard
0.55	The previous landslides have occurred locally. Several landslides have occurred under certain conditions.	Moderate hazard
0.30	Landslide occurrence probability is low and slopes are generally stable.	Low hazard
0.10	Landslide occurs rarely or it does not exist at all. Slopes are naturally stable.	Very low hazard

Table 4. Linguistic rules for risk scoring of different resource types [32, modified]

Fuzzy membership value for resource damage potential	Linguistic rules for risk scoring	Resource types
1	It has a direct impact on the residents. Major damages are as killed, wounded and financial losses.	Residential area
0.90	The road network is affected by landslides. Major damages are including: disconnection in the area can effect on the rescue and rehabilitation operations after the disaster.	Road
0.70	It has a direct impact on the financial situation of individuals and essential foods.	Irrigated field
0.35	It has a direct impact on the economy of local residents.	Non-irrigated farmland
0.80	It has a direct impact on the economy and people's feeding.	orchards
0.60	It has a direct impact on the financial situation of individuals; in addition, it causes the loss of national resources.	Rangeland
0.30	National resources are destroyed, but it has no a direct impact on the individual economy of residents.	Forested land

Given two maps with fuzzy membership, functions can be employed to combine membership values [84]. Several fuzzy operators exist for combining membership functions. The applied fuzzy operators have much dependence on the type and nature of combined spatial data [85, 86]. In this study, the membership values of LHP and RDP have been combined using fuzzy algebraic product operator and landslide risk was calculated per pixel in the region. The operator of fuzzy algebraic product has been expressed mathematically as:

$$\mu_{PRODUCT}(x)=\prod_{i=1}^{2}\mu_i(x) \quad (11)$$

The obtained matrix values were divided into five vulnerable groups (Table 5), that result has been shown in a landslide risk map. The software packages used were ArcGIS -10.3 and SPSS Statistics Version 22.

Table 5. The classes boundaries of landslide risk values [32]

Landslide risk zones	Landslide risk rates
Very low risk (VLR)	0.1 ≥Landslide risk>0.0
Low risk (LR)	0.2≥Landslide risk>0.1
Moderate risk (MR)	o.4≥Landslide risk>0.2
High risk (HR)	0.6≥Landslide risk> 0.4
Very high risk (VHR)	0.6<Landslide risk

4- Results

4- 1- Causal factors

The mapping of the study area at scale 1:25000 has produced a number of interesting results. The role of marly formation and altered zones, due to the presence of clay minerals, are very important in the occurrence of landslides [87]. The swelling potential rates of the marly and clayey samples of landslide area have been evaluated using physical and chemical properties of soils [88]. In the study region, the inherent properties of the soils that have clay minerals show that these soils have a medium to high swelling potential [89]. According to the physical and chemical assessment criteria at least 80% of the clayey material in the area have a swelling potential with medium to high intensity and soils at the unstable slopes are inherently "expansive soils", where landslide can occur even without human intervention [90, 91]. The soil with clay minerals especially Montmorillonite could be the main reason of the landslide occurrence because of swelling and shrinkage characteristics at various moisture contents [92-94]. In the study area, marly and clayey formations with high-plasticity expansive materials are associated with numerous slope instability [95]. The type of lithology, due to their impact on rocks and soil resistance and permeability, are considered one of the most important factors in landslide occurrence [50, 53, 54]. Due to variations in the geological formations of the region and various degrees of sensitivity of the rocks to landslide, lithology also plays an important role in spread of landslides in the region [11-13]. Petrographically, the rocks range from Late Precambrian to Recent [96] and could be divided into a number of distinct group including calcareous rocks, plutonic, volcanic and pyroclastic rocks, metamorphic as well as sedimentary deposits of Neogene age, metamorphic rocks and quaternary sediments (Figure 7). About 32.8% of the whole area of the Miocene epoch clayey and marly sedimentary rocks and 42.97% of the whole area of altered zones had experienced landslides [11, 13, 95]. This rate of landslide is remarkable compared to other lithologies. The results obtained from the contingency tables revealed that the highest number and area of landslides occurred on Miocene clay to marly sedimentary rocks [13]. Therefore, the effect of expansive soils is now generally accepted in slope instability [91].

The range of failure depths change between 5 to 25 m, with a mean value of about 10 m. Most of these landslides affect lithologic units composed by marls, alteration zones, volcanic rock and regolith[1]. The term marl has been assigned various meaning. It has been defined as a rock with 35-65% clay and a complementary content of carbonate [97]. It can be concluded that the marl formations of the area are considered as hard soil and soft rock [98]. During the field studies carried out for the preparation of landslide inventory maps, it was found that most springs that led to slope instabilities in the region are located at the boundary between the impermeable sedimentary units of Neogene age (mostly marls, mudstone, siltstone, sandstone, conglomerate and altered zones) and semi-permeable igneous rocks with joints and fractures of Eocene age. Field checking indicates that the failures generally occurred in the marly sediments and along the sedimentary-volcanic rock contact surfaces. Rapid changes in water levels during late winter or early spring rainfalls cause new landslides or reactivation of the old landslides in these times [90]. There are seven basic types of landslides that occur in three types of material. Flows, translational, rotational slides combinations of translational-rotational, creep, unmappable and widespread can occur in bedrock, debris, soils or a combination of the soil and rock. The soil materials are related with the 73% of landslides occurred in the study area. [10, 11, 13, 99].

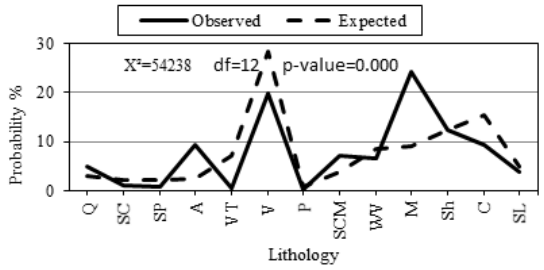

Figure 7. Landslide probability histogram and chi-square test result based on lithological and landslide maps

The results of the spatial relationship analysis between distance from faults and landslide show that approximately 75% of landslides are distributed within 0-8 km from the major faults. Moreover, movement along an existing fault, e.g. caused by earthquake, can also trigger landslides. The major land use classes in the area are rangeland (> 92%), farmland and orchard (5.2%), forest (2%) and build-up area. Vegetation provides both hydrological and mechanical effects that generally are advantageous to stability of the slopes. Comparing aerial photographs of the years 1958, 1968 and 1993 with 2002 satellite images shows that in this period, many changes have taken place in land use/land cover types in the area. For more than 55 years, the forest and rangelands have been extensively damaged due to unprincipled actions and applications or have been changed into agricultural lands, orchards, and build-up areas or used to construct roads. It is quite difficult to find an area that is unaffected by these changes. Landslide occurs 2 to 6 times more in agricultural areas, orchards, sparse forests and some poor rangelands than in other land uses. In contrast, in the forest with deep root trees and pristine rangelands, the slopes have good stability. Investigations of landslide inventory maps and field studies revealed that occurrence of landslides in lands with a use change has increased 6 times over the past 55 years.

Groundwater aquifers are mainly found in calcareous sedimentary rocks in the eastern parts as well as in non-carbonate sedimentary strata comprising marl, mudstone,

1 is a layer of loose, heterogeneous superficial deposits covering solid rock

siltstone, sandstone, conglomerate, and volcanic rocks, which include lavas and tuffs located mostly in the western part of the region. With respect to the relative permeability, the lithology units in the study area can fall into three groups: permeable, semi-permeable and impermeable [100] (Figure 8). Analysis of the relationship of landslide occurrence with rock types show that the most of landslides have occurred in impermeable areas (Table 6). During the field studies carried out for the preparation of landslide inventory maps, it was found that most springs that led to slope instabilities in the region are located at the boundary between the impermeable and semi-permeable lithologies. Field checking indicates that the failures generally occurred along the sedimentary-volcanic rock contact surfaces. Rapid changes in water levels during intense rain showers cause new landslides or reactivation of the old landslides in these times [90].

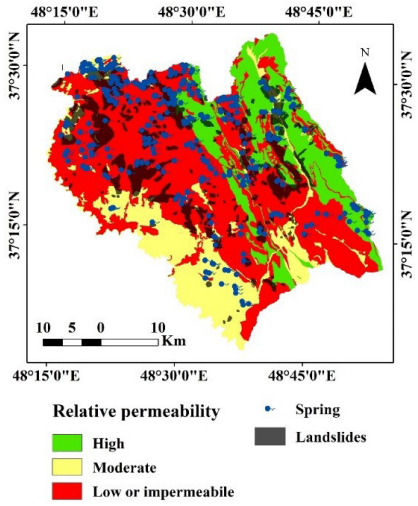

Figure 8. Relative permeability map of the lithologies [90]

An increase in the amount of rainfall together with the increase in river discharge accelerate the erosion along river banks; which boosts the slop failures [33, 101]. The results of present study suggest that slopes closer to the stream lines are more affected than remote ones. In the study area, stream bank erosion has been responsible for 81% of single landslides and 42% of landslide zones. The probability of landslide occurrence on Northeast facing slope is about 2.25 times more than other slope aspects in the study area. Northeast facing slopes in direct contact with the humid airflow from the Caspian Sea have more rainfall and higher humidity, when compared with those to the other slope aspects.

Slope angle is considered the most important factor in the slope failures [43, 102], it is expected that by increase in the slope gradient the landslide hazard potential is increased as well [56]. Slope angles in the study area ranged from 0° to 73°, while landslide density is high (68.85%) for slopes with gradients 10 and 30 degree. The lithology and gradient of slopes are dependent [54] and in most areas, gradient increase in the slope cannot be the only landslide controller [103]. Lithology and slope gradients are the most influential factors for landslide occurrence in the study area. In the slopes with susceptible lithology (marl and clay sedimentary formations and altered zones) and gentle grade (slopes with gradients from 10–30°), the penetration of water can be considered as effective factor in the event of widespread landslides [104]. The relief developed is very marked and range from 850 m in the Qezel Owzan River in the southwestern corner of the area to 3324 m at the peak of the Agh Dagh that is the heighest point in the study area. Landslides between 1000 m to 2200 m are dominant (90.5%) due to the lithological character of the layers that have marl and clay compositions. Most of rock outcrop of formations susceptible to landslides such as altered rocks, marl and clay sedimentary rocks correspond to the slopes with elevation of 1,000 to 2,200 meters and provide favorable conditions for rainfall infiltration; these conditions can be effective in the landslide occurrence. A total of 50.4% of the study area was concave slopes (-1), 48.4% was convex slopes and 1.3% was flat, their respective frequency ratios were 0.106, 0.111 and 0.129, indicating nearly a same likelihood of landslide occurrence. According to PGA map, about 98.8% of the past landslide areas fall in high Peak Ground Acceleration zones (0.57 and 0.58 (g)).

4- 2- Landslides susceptibility and hazard analysis

In this paper, landslide probability was calculated using categorical and continuous variables. Explanatory factors were introduced into favorability functions model as independent variables. Based on Equation 6, the two ratio function have been estimated, one for the five continuous independent variables: distance to fault lines, distance to drainage network, slope gradient, distance to roads and distance to settlement, and the other for the five categorical independent variables: lithology, land-use/land cover, elevation, slope aspect and slope curvature separately. Based on Equation 7, the estimated value for $\lambda\gamma(x_1,\ldots,x_k,y_1,\ldots,y_h)$ were normalized in a specific range, between 0 and 1. The result is a raster map with the pixel values representing the relative probability of landslide occurrence (Figure 9a). The probability values of landslide occurrence have been divided into five classes by using standard deviation method to produce a LSM of region with five classes as very low susceptible (VLS), low susceptible (LS), moderate susceptible (MS), high susceptible (HS) and very high susceptible (VHS) (Figure 9b). Based on the result of the obtained landslide susceptibility map, 77.4% of the total area show low and very low landslide susceptibility. Moderate, high and very high susceptible zones make up 8.5% and 14.2% of the total area, respectively.

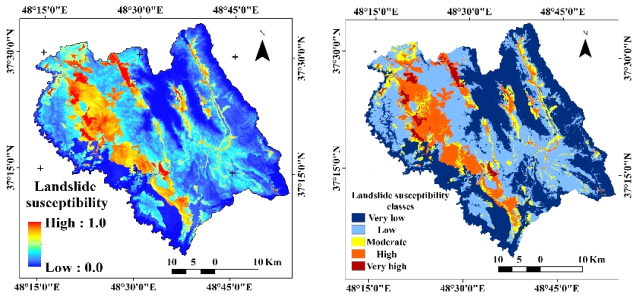

Figure 9. a) Landslide susceptibility and b) its different classes in the region

Table 6. Landslide densities of the relative permeability classes in the study area

Relative permeability	Grid cells (pixels) with landslide		All grid (pixels) cells		Landslide density (%)
	Frequency (no. of pixels)	%	Frequency (no. of pixels)	%	
Low or impermeable	57164	73.8	419072	59.2	13.64
Moderate (semi-permeable)	10008	12.9	146907	20.7	6.8
High (permeable)	10275	13.3	142477	20.1	7.2

LSM, the annual mean precipitation and PGA maps were overlaid to provide a landslide hazard map. Before overlying the triggering factors and landslide susceptibility layer, they must be normalized to a common dimensionless scale. To perform this process, the Equation 7 was used and the result is a raster layer with the pixel values, which vary from 0 to 1 (Figure 10a). In the new map zero represents minimal hazard and 1 represents maximum hazard of landslides in the area. Based on the results of the landslide hazard modeling and with respect to Figure 8a, it is possible to determine the hazard level for any point on a map. LHM was classified into five categories e.g. very low, low, moderate, high and very high (Figure 10b). Based on the result of the obtained landslide hazard map, 78.1% of the total area show low landslide hazard. Moderate, high and very high hazard zones make up 8.6% and 13.3% of the total area, respectively.

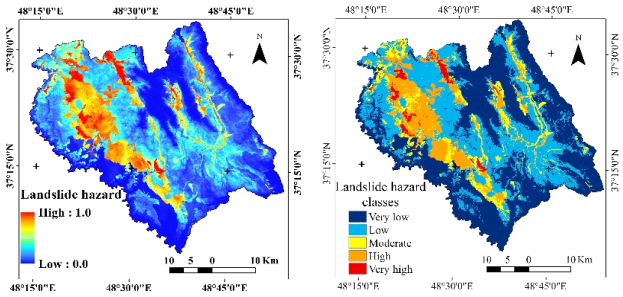

(a) (b)

Figure 10. a) Landslides hazard and b) different levels of hazard

The Area Under Curve (AUC) value of ROC curve for landslide susceptibility model is 0.849 and the prediction accuracy of the model is 84.9% (Figure 11a). This result shows that there is a good agreement between the prediction accuracy and the landslides occurrence in the region [67, 105, 106]. The ROC curve for landslide hazard model used in this study is given in Figure 11b. The AUC value for the hazard map obtained is 0.848, equivalent to an accuracy of 84.8%. The result shows that there is a fair agreement the hazard prediction accuracy and the landslide occurrence in study region. Such a result indicates that the landslide hazard model has a stable and good prediction performance.

4- 3- Landslide Risk Assessment

Landslide risk is considered as a function of LHP and RDP. Landslide risk values for different combinations of RDP and LHP can be shown in the form of a LRA matrix, as given in Table 7. Landslide risk was calculated in each pixel by multiplying the LHP value and RDP.

As it is observed from matrix of LRA, the LRA value for each pixel range from 0.03 to 1.0. The value of 0.03 represents a very small landslide risk potential in forestlands while the value of 1 indicates very high landslide risk potential in habitat areas. To aid visual interpretation, landslides risk values between 0.03 and 1.0 were divided into five landslide risk classes as per the scheme given in Table 5. Based on this method, the risk classes were defined as very high risk (VHR), high risk (HR), moderate risk (MR), low risk (LR), and very low risk (VLR) (Figure 12).

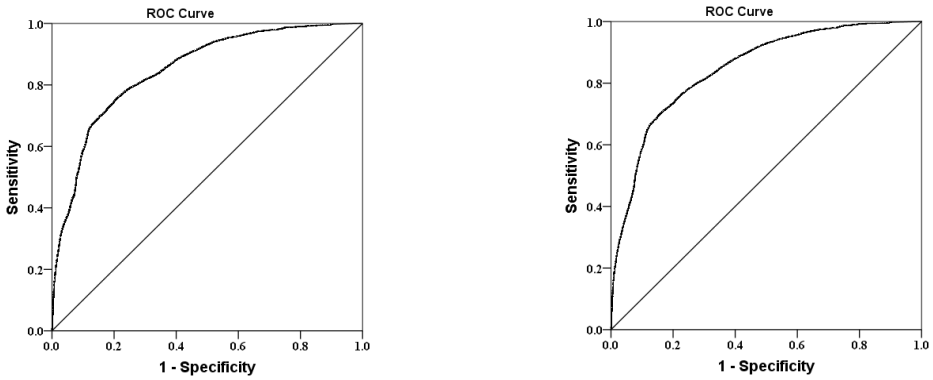

(a) (b)

Figure 11. ROC curve to evaluate the accuracy of the model [Author]: a) susceptibility of the area under the curve 0.849 and b) hazard with AUC 0.848

Table 7. Landslide risk assessment matrix for various combinations of the LHP and RDP. Red: very high hazard; Pink: high hazard; Yellow: moderate hazard; Blue: low hazard; Green: very low hazard [32, modified].

Resource damage potential (RDP)	Landslide hazard potential (LHP)				
	Very high hazard (VHH) (1.00)	High Hazard (HH) (0.80)	Moderate Hazard (MH) (0.55)	Low hazard (LH) (0.30)	Very low hazard (VLH) (0.10)
Residential area (1.00)	1.00	0.8	0.55	0.30	0.10
Roads (0.90)	0.90	0.72	0.50	0.27	0.09
Garden (0.80)	0.80	0.64	0.44	0.24	0.08
Irrigated field (0.70)	0.70	0.56	0.38	0.21	0.07
Rangeland (0.60)	0.60	0.48	0.33	0.18	0.06
Non-irrigated farmland (0.35)	0.35	0.28	0.19	0.10	0.03
Forested land (0.30)	0.30	0.24	0.16	0.09	0.03
Very high risk	High risk	Moderate risk	Low risk	Very low risk	

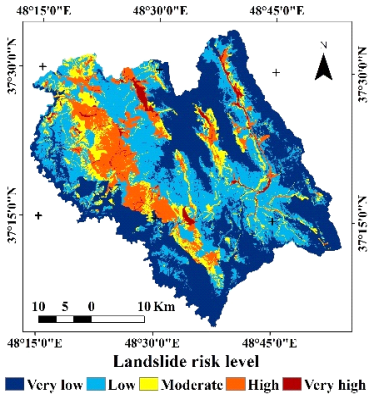

Figure 12. The landslides risk levels in the study area [Author]

According to this risk map, 13.8% of the study area falls in the high and very high landslide risk zones. The very high landslide risk area is 2.3% of the total study area. The moderate-, low- and very low landslide risk zones form 8%, 21.5% and 56.6% of the area, respectively. About 62.5% of the orchard land, 54.4% of agricultural land,41.5% of the residential areas and 27.7% of the area with a road are estimated to be high and very high risk. Based on the results only 11.6% of the rangelands are located in high and very high-risk classes. The main area of zones with low and very low risk have moderate or good rangeland cover.

5- Discussion

Landslides are the most common natural disaster seen in the studied area in the Alborz mountain, NW-Iran. The occurrence of new landslides as well as reactivation of old ones in the region have caused significant damages to natural resources, agricultural fields, buildings and infrastructure over the past 55 years. The main aim of this paper was to design a methodology for the assessment of landslide susceptibility, hazard and risk as basic information for risk prevention and landuse planning in the region of NW Iran. The present study contributes to the debate on the LRA. Based on LRA map, a risk management procedure can be proposed to reduce the possible risk to elements available in the study region. Landslide risk analysis in a regional scale requires a complex multi-step process, and to this aim, it is essential to have landslide hazard layer and damage potential of the elements at risk [45]. The results from the study region suggest that the combined approach is effective in landslide susceptibility, hazard and risk assessment and can be extrapolated to another study area and the developed method can be used in basin scale projects.

In international landslide literature, it is possible to find many studies on LSA [22, 35-37, 48, 53, 76, 105, 107, 108]. However, only limited research has been done on LRA for large area such as south of Ardabil province region [22, 109]. In this study, a raster based combined model on a regional scale was developed using a spatial prediction method and the fuzzy sets theory to landslide susceptibility, hazard and risk assessment. The first stage of our study involved collecting a detailed landslide inventory data in the study area for a 55-year-long period (1960-2015). Landslide susceptibility was determined for the area and the generated data constituted a base to assess landslide hazard in the region. Adequate data in this area have allowed the estimation of annual rainfall and calculation of PGA. Accordingly, the conversion of LSM to LHM became possible using precipitation and seismicity data. LRA map was prepared by combination of RDP and LHP. The risk map resulted from the study was classified in the form of zones with very high risk, high risk, moderate risk, low risk and very low risk degrees. According to the risk map obtained from proposed model, 13.8% of the area is located in zones with high and very high-risk classes.

The landslide risk evaluation becomes further complicated in many regions due to the insufficient historical records on landslides, unavailability of input data on past losses and the uncertainty in the assessment of landslide risk [110]. Uncertainties in estimation of landslides intensity,

transformation of LSM into a hazard model and determining of the LHP and RDP of elements at risk constitute the main limitations for landslide hazard and risk studies [44]. High-quality input data and determination of suitable factors are crucially important for the landslide susceptibility and hazard assessment of the study region. Uncertainty associated to errors of landslide inventory, data collection, database generation, factors affecting the occurrence of landslides and their propagation on landslide susceptibility and hazard assessment results are evaluated by Area Under Curve of ROC curve method. Based on the Area Under Curve of ROC curve (AUC), the prediction ability of the model is 84.9%, which is a good result for prediction of the landslide susceptibility in the study region. Therefore, the LSM can be transformed to LHM with an acceptable accuracy. Landslide hazard model has been validated by ROC curve analysis, which has given 84.8% accuracy. These results suggest a good performance of the used methods. Therefore, the landslide risk map produced by using this LHM with high precision as a LHP layer yield a higher accuracy and higher certainty.

Landslides susceptibility and hazard were evaluated at a pixel basis by correlation between specified types of past landslides (moderate to high intensity landslides occurred or reactivated at least once over the last 55 years) and a set of independent factors, which controls the instability. The twelve probable landslide-causing factors used in the landslide susceptibility and hazard evaluation have a high relevance and a low uncertainty association [7]. Historical data derived from the landslides frequency-intensity relationship cannot be completely reliable criterion to determine future landslide activity [111]. Therefore, review of the past decades reveals that more than 60% of landslides chosen to implement the model in the region are active now and this can somewhat reduce the foregoing uncertainties.

Implementation of the model in pixel units can reduce the accuracy of the calculations due to the non-geometrical shape of landslides, but selecting pixels of 50m×50m on a regional scale has reduced the uncertainty [17]. The smallest area of landslide is approximately 15805 m^2, which is more than six times the size of the pixels (2,500 m^2). In the proposed approach, the LHP levels and classes of RDP have been quantified in terms of fuzzy membership values as per their relative importance to risk analysis. There are several inherent uncertainties in the methodology as well as in assessment of the LHP and RDP. The first one arises from the empirical nature of the assessment. The accuracy of the predictive model of landslide hazard is 84.8%, which is a very good result for LHP preparation purposes. The second one concerns accuracy, nature and quality of data on damages to different resources at risk from landslides. In the present study, the database of elements at risk was used to assess the damage potential of different resources. Clearly, the higher quality the data will have the more accurate the results of the assessments. A complete and detailed inventory of elements at risk was carried out in order to reduce uncertainty in the RDP assessment procedure.

6- Conclusions

For the first time, in this study, LRA was accomplished on a regional scale for southern part of Ardabil province by using a combined method; which makes it the single landslide risk management study ever to be carried out in the West of Alborz mountain range located in the Northwest of Iran. The accuracies of the landslide susceptibility and hazard maps are 84.9%, and 84.8% respectively. This results indicate that the models are useful and suitable for the regional scale adopted in this study. According to the risk map obtained from proposed model, of the area considered in the present study, 13.8% falls in the high and very high-risk zones. About 62.5% of the orchard lands and 54.4% of agricultural lands are located in areas with high and very high-risk zones. About 41.5% of settlement areas and 27.7% of the area with a road are estimated to be high and very high risk. Based on the results only 11.6% of the rangelands are located in high and very high risk. In these slopes, the rangeland coverage is either destroyed or severely weakened due to in discriminate exploitation. The main area of zones with low and very low risk have moderate or good rangeland cover. In the high risk zone, we should avoid the construction of any construction for human and livestock settlement. In cases where the building has already been made then the extension or rebuilding of it should be avoided. If forced to do construction activity in these areas, the necessary measures should be taken to reduce risk in slopes. This model can be used to evaluate landslide risks in similar mountainous areas such as Zagros and Alborz Mountain Ranges in Iran and mountain ranges in Caucasus.

References

[1] Intarawichian, N. and Dasananda, S. (2010). Analytical hierarchy process for landslide susceptibility mapping in Lower Mae Chaem watershed, Northern Thailand. Suranaree Journal of Science and Technology, 17(3): 277-292.

[2] Raghuvanshi, T.K., Ibrahim, J. and Ayalew, D. (2014). Slope stability susceptibility evaluation parameter (SSEP) rating scheme – An approach for landslide hazard zonation. Journal of African Earth Sciences, 99: 595–612.

[3] Budimir, M.E.A., Atkinson, P.M. and Lewis, H.G. (2015). A systematic review of landslide probability mapping using logistic regression. Landslides, 12: 419–436.

[4] Kojima, H., Chung Chang-Jo, F. and van Westen, C.J. (2000). Strategy on the landslide type analysis based on the expert knowledge and the quantitative prediction model. International Archives of Photogrammetry and Remote Sensing, XXXIII, B7: 701-707.

[5] Shoaei, Z., Shoaei, G. and Emamjomeh, R. (2005). Interpretation of the mechanism of motion and suggestion of remedial measures using GPS continuous monitoring data In: Landslides: Risk analysis and sustainable disaster management. Sassa, K., Fukuoka, H., Wang, F. and Wang, G., (eds.), Proceeding of the first general assembly of the international consortium of landslides. Springer, p. 327-335.

[6] Komakpanah, A. and Hafezimoghadasi, N. (1994). Landslide hazard zonation methods. 1th workshop proceeding on landslide damage mitigation strategies in Iran. Scientific Report, International Institute of Earthquake Engineering and Seismology, p. 390-414 (in Persian).

[7] Talaei, R., (2011). Geological study and landslide hazard (risk) assessment in Hashtchin area (Ardabil Province of Iran), [PhD Thesis]. Faculty of geology, Baku State University. Baku, Azerbaijan, 247p. (in Azerbaijani).

[8] Ansari, F. and Blurchi, M.C. (1996). Landslides of Ardabile Province, Iran. Geological survey of Iran, Iran. 46p. (in Persian).

[9] Nikandish, N. and Mir Sanei, R. (1996). Introduction to Ardabile Province landslides. Iran Ministry of Jihad-e-Agriculture, Tehran, Iran. 63p. (in Persian).

[10] Hashemi Tabatabaei, S. (1998). Landslide hazard zonation in southwest of Ardabil Province Iran. Scientific and Technical Report, The center for building and housing researches. Department of Housing and Urban Development of Ardabil, Ministry of Roads and Urban Development, Tehran, Iran. Vol. 2, p. 25-72 (in Persian).

[11] Mahdavifar, M.R. (1997). Landslide hazard zonation in Khorshrostam region (southwest of Khalkhal County). MSc Dissertation,Tarbiat Modarres University, Tehran, Iran. 154p. (in Persian).

[12] Uromeihy, A. and Mahdavifar, M.R. (2000). Landslide hazard zonation of the Khorshrostam area, Iran. Bulletin of Engineering Geology and the Environment, 58: 207-213.

[13] Talaei, R., Ghayoumian, J., Shariat Jafari, M. and Aliakbarzadeh, E. (2004). Study on effective factor causing landslide in southwest of Khalkhal region. Agriculture research and education organization, Ministry of Jahad-e-Agriculture. Tehran, Iran. 153p. (in Persian).

[14] Martha, T.R., van Westen, C.J., Kerle, N., Jetten, V. and Kumar, K.V. (2013). Landslide hazard and risk assessment using semi-automatically created landslide inventories. Geomorphology, 184: 139–150.

[15] Sinarta, N., Rifái, A., Fathani, T.F. and Wilopo, W. (2017). Slope stability assessment using trigger parameters and SINMAP methods on Tamblingan-Buyan ancient mountain area in Buleleng Regency, Bali. Geosciences, 7, 110: 16 pages. www.mdpi.com/journal/geosciences

[16] Nsengiyumva, J.B., Luo, G., Nahayo, L., Huang, X. and Cai, P. (2018). Landslide susceptibility assessment using spatial multi-criteria evaluation model in Rwanda. Int. J. Environ. Res. Public Health, 15, 243: 23 pages. www.mdpi.com/journal/ijerph.

[17] Camilo, D.C., Lombardo, L., Mai, M.P., Doud, J. and Husera, R. (2017). Handling high predictor dimensionality in slope-unit-based landslide susceptibility models through LASSO-penalized Generalized Linear Model. Environmental Modelling & Software, 97: 145-156.

[18] Schlögel, R., Marchesini, I., Alvioli, M., Reichenbach, P., Rossi, M. and Malet, J.-P. (2018). Optimizing landslide susceptibility zonation: Effects of DEM spatial resolution and slope unit delineation on logistic regression models. Geomorphology, 301: 10-20.

[19] Jaiswal, P., van.Westen, C.J. and Jetten, V. (2010). Quantitative assessment of direct and indirect landslide risk along transportation lines in southern India. Nat. Hazards Earth Syst. Sci., 10: 1253–1267.

[20] Lari, S., Frattini, P. and Crosta, G.B. (2014). A probabilistic approach for landslide hazard analysis. Engineering Geology, 182(Part A): 3-14.

[21] Lee, E.M. and Jones, D.K.C. (2004). Landslide risk assessment. Thomas Telford, London, 454 p.

[22] Yoshimatsu, H. and Abe, S. (2006). A review of landslide hazards in Japan and assessment of their susceptibility using an analytical hierarchic process (AHP) method. Landslides, 3: 149–158.

[23] van Westen, C.J., van Asch, T.W.J. and Soeters. R. (2006). Landslide hazard and risk zonation- why is it still so difficult? Bulletin of Engineering Geology and the Environment, 65:176–184.

[24] Liu, X., Yu, C., Shi, P. and Fang, W. (2012). Debris flow and landslide hazard mapping and risk analysis in China. Front. Earth Sci., 6(3): 306–313.

[25] Bonnard, C., Forlati, F. and Scavia C. (2004). Identification and mitigation of large landslide risk in Europe. Advances in risk assessment. Imiriland project. A.A. Balkema, Leiden, London, 317p.

[26] Eberhardt, E., Thuro, K. and Luginbuehl, M. (2005). Slope instability mechanisms in dipping interbedded conglomerates and weathered marls-the 1999 Rufi landslide, Switzerland. Engineering Geology, 77:35–56.

[27] Cardinali, M., Reichenbach, P., Guzzetti, F., Ardizzone, F., Antonini, G., Galli, M., Cacciano, M., Castellani, M. and Salvati, P. (2002). A geomorphological approach to estimate landslide hazard and risk in urban and rural areas in Umbria, central Italy. Natural Hazards and Earth Systems Science, 2(1–2): 57–72.

[28] Shou, K.J. and Chen, Y.L. (2005). Spatial risk analysis of Li-shan landslide in Taiwan. Engineering Geology, 80: 199-213.

[29] Bell, R. and Glade, T. (2004). Quantitative risk analysis for landslides – Examples from Bíldudalur, NW-Iceland. Natural Hazards and Earth System Sciences, 4: 117-131.

[30] Corominas, J., van Westen, C., Frattini, P., Cascini, L., Malet, J.P., Fotopoulou, S., Catani, F., Van Den Eeckhaut, M., Mavrouli, O., Agliardi, F., Pitilakis, K., Winter, M.G., Pastor, M., Ferlisi, S., Tofani, V., Hervάs, J. and Smith, J.T. (2014). Recommendations for the quantitative analysis of landslide risk. Bull Eng Geol Environ, 73: 209–263.

[31] Sajinkumar, K.S., Anbazhagan, S., Rani, V.R. and Muraleedharan, C. (2014). A paradigm quantitative approach for a regional risk assessment and management in a few landslide prone hamlets along the windward slope of Western Ghats, India. International Journal of Disaster Risk Reduction, 7: 142–153.

[32] Kanungo, D.P., Arora, M.K., Gupta, R.P. and Sarkar, S. (2008). Landslide risk assessment using concepts of danger pixels and fuzzy set theory in Darjeeling Himalayas. Landslides, 5: 407–416.

[33] Fourniadis, I.G., Liu, J.G. and Mason, P.J. (2007). Landslide hazard assessment in the Three Gorges area, China, using ASTER imagery: Wushan–Badong. Geomorphology 84: 126–144.

[34] Yalcin, A. (2008). GIS-based landslide susceptibility mapping using analytical hierarchy process and bivariate statistics in Ardesen (Turkey): Comparisons of results and confirmations. Catena, 72:1–12.

[35] Chu, C.M., Tsai, B.W. and Chang, K.T. (2009). Integrating decision tree and spatial cluster analysis for

landslide susceptibility zonation. World Academy of Science, Engineering and Technology, 59: 479-483.

[36] Dragićević, S., Carević, I., Kostadinov, S., Novković, I., Abolmasov, B., Milojković, B. and Simić, D. (2012). Landslide susceptibility zonation in the Kolubara river basin (western Serbia) - analysis of input data. Carpathian Journal of Earth and Environmental Sciences, 7(2): 37-47.

[37] Zizioli, D., Meisina, C., Valentino, R. and Montrasio, L. (2013). Comparison between different approaches to modeling shallow landslide susceptibility: a case history in Oltrepo Pavese, Northern Italy. Natural Hazards and Earth System Sciences, 13: 559–573.

[38] Greco, R., Sorriso-Valvo, M. and Catalano E. (2007). Logistic regression analysis in the evaluation of mass movements susceptibility: the Aspromonte case study, Calabria, Italy. Engineering Geology, 89: 47–66.

[39] Grozavu, A., Mărgărint, M.C. and Patriche C.V. (2012). Landslide susceptibility assessment in the brăieşti-sineşti sector of iaşi cuesta. Carpathian Journal of Earth and Environmental Sciences, 5 (2): 61-70.

[40] Oh, H.J., Lee, S. (2017). Shallow landslide susceptibility modeling using the data mining models artificial neural network and Boosted Tree. Appl. Sci., 7(1000): 1-14.

[41] Hemasinghe, H., Rangali, R.S.S, Deshapriya, N.L. and Samarakoon, L. (2018). Landslide susceptibility mapping using logistic regression model (a case study in Badulla District, Sri Lanka). Procedia Engineering, 212: 1046–1053.

[42] Mathew, J., Jha, V.K. and Rawat, G.S. (2009). Landslide susceptibility zonation mapping and its validation in part of Garhwal Lesser Himalaya, India, using binary logistic regression analysis and receiver operating characteristic curve method. Landslides, 6: 17–26.

[43] Shit, P.K., Bhunia, G.S. and Maiti, R. (2016). Potential landslide susceptibility mapping using weighted overlay model (WOM). Model. Earth Syst. Environ, 2:21, 1-10.

[44] Akgun, A., Kıncal, C. and Pradhan, B. (2012). Application of remote sensing data and GIS for landslide risk assessment as an environmental threat to Izmir city (west Turkey). Environ. Monit. Assess, 184: 5453–5470.

[45] Zêzere, J.L., Garcia, R.A.C., Oliveira, S.C. and Reis, E. (2008). Probabilistic landslide risk analysis considering direct costs in the area north of Lisbon (Portugal). Geomorphology, 94: 467–495.

[46] Nefeslioglu, H.A., Gokceoglu, C., Sonmez, H. and Gorum, T. (2011). Medium-scale hazard mapping for shallow landslide initiation: The Buyukkoy catchment area (Cayeli, Rize, Turkey). Landslides, 8(4): 459-483.

[47] van Westen, C.J., Castellanos, E. and Kuriakose, S.L. (2008). Spatial data for landslide susceptibility, hazard, and vulnerability assessment: An overview. Engineering Geology, 102: 112-131.

[48] Bălteanu, D., Chendeş, V., Sima, M. and Enciu, P. (2010). A country-wide spatial assessment of landslide susceptibility in Romania. Geomorphology, 124: 102–112.

[49] Duruturk, B., Demir, N., Koseoglu, I., Onal, U.B. and Ercanoglu, M. (2017). Gis-based determination of landslide properties in regional scale: Karabuk province (NW Turkey). Annals of Valahia University of Targoviste. Geographical Series, 17(1): 37-46.

[50] Lan, H.X., Zhou, C.H., Wang, L.J., Zhang, H.Y. and Li, R.H. (2004). Landslide hazard spatial analysis and prediction using GIS in the Xiaojiang watershed, Yunnan, China. Engineering Geology, 76: 109–128.

[51] Guzzetti, F., Carrara, A., Cardinali, M. and Reichenbach, P. (1999). Landslide hazard evaluation: a review of current techniques and their application in a multi-scale study, Central Italy. Geomorphology, 31: 181–216.

[52] Wang, H.B. and Sassa, K. (2005). Comparative evaluation of landslide susceptibility in Minamata area, Japan. Environmental Geology, 47: 956-966.

[53] Ayalew, L. and Yamagishi, H. (2005). The application of GIS-based logistic regression for landslide susceptibility mapping in the Kakuda-Yahiko Mountains, Central Japan. Geomorphology, 65: 15–31.

[54] Saldivar-Sali, A. and Einstein, H.H. (2007). A Landslide risk Rating System for Baguio, Philippines. Engineering Geology, 91(2-4): 85-99.

[55] Knapen, A., Kitutu, M.G., Poesen, J., Breugelmans, W., Deckers, J. and Muwanga, A. (2006). Landslides in a densely populated county at the footslopes of Mount Elgon (Uganda): Characteristics and causal factors. Geomorphology, 73: 149–165.

[56] Gómez, H. and Kavzoglu, T. (2005). Assessment of shallow landslide susceptibility using artificial neural networks in Jabonosa River Basin, Venezuela. Engineering Geology, 78: 11 –27.

[57] Dai, F.C., Lee, C.F. and Ngai, Y.Y. (2002). Landslide risk assessment and management: an overview. Engineering Geology, 64 (1): 65– 87.

[58] Kouli, M., Loupasakis, C., Soupios, P. and Vallianatos, F. (2010). Landslide hazard zonation in high risk areas of Rethymno Prefecture, Crete Island, Greece. Natural Hazards, 52(3): 599–621.

[59] Hemmati, R., Dolatimehr, A., Nasirifar, A., Shahbazi, M., Hezhabrpour, Gh. and Aghaei. Kh. (2007). Ardabil Province climate. Scientific and Technical Report, Applied Meteorology research center of Ardabil, Islamic Republication of Iran Meteorological Organization, Ministry of Roads and Urban Development, Iran, 143p. (in Persian).

[60] Williams, J.G., Rosser, N.J., Kincey, M.E., Benjamin, J., Oven, K.J., Densmore, A.L., Milledge, D.G., Robinson, T.R., Jordan, C.A. and Dijkstra, T.A. (2018). Satellite-based emergency mapping using optical imagery: experience and reflections from the 2015 Nepal earthquakes. Nat. Hazards Earth Syst. Sci., 18: 185–205.

[61] Liu, L., Xu, C., Xu, X., Tian, Y., Ran, Y. and Chen, J. (2015). Interactive statistical analysis of predisposing factors for earthquake-triggered landslides: a case study of the 2013 Lushan, China Ms7.0 earthquake. Environ Earth Sci, 73:4729–4738.

[62] Ghorashi, M. and Berberian, M. (1992a) The Rudbar-Tarom earthquake of 20 June 1990 in NW Iran: A preliminary field reconnaissance report. Scintific Quarterly Journal, GeoSciences, 1(1): 16-29 (in Persian).

[63] Ghorashi, M. and Berberian, M. (1992b). The Rudbar-Tarom earthquake of 20 June 1990 in NW Iran: A preliminary field reconnaissance report. Scintific Quarterly Journal, GeoSciences, 1(2): 6-17 (in Persian).

[64] Deniz, A., Korkmaz, A.K. and Irfanoglu, A. (2010). Probabilistic seismic hazard assessment for İzmir, Turkey. Pure and Applied Geophysics, 167: 1475–1484.

[65] Frankel, A., Mueller, C., Barnhard, T., Perkins, D., Leyendecker, E., Dickman, N., Hanson, S. and Hopper, M. (1996). National seismic hazard maps: documentation June 1996. USGS Open-File Report, 96-532,70 pages.

[66] Wang, Z. (2006). Understanding seismic hazard and risk assessments: an example in the New Madrid seismic zone of the central United States. Proceedings of the 8th U.S. National Conference on Earthquake Engineering April 18-22, 2006, San Francisco, California, USA. Paper No. 416. 11 pages.

[67] Sdao, F., Lioi, D.S., Pascale, S., Caniani, D. and Mancini, I.M. (2013). Landslide susceptibility assessment by using a neuro-fuzzy model: a case study in the Rupestrian heritage rich area of Matera. Natural Hazards and Earth System Sciences, 13: 395–407.

[68] Conforti, M., Pascale, S., Robustelli, G. and Sdao, F. (2014). Evaluation of prediction capability of the artificial neural networks for mapping landslide susceptibility in the Turbolo River catchment (northern Calabria, Italy). Catena, 113: 236–250.

[69] Chung, C.J. (2006). Using likelihood ratio functions for modeling the conditional probability of occurrence of future landslides for risk assessment. Computers and Geosciences, 32: 1052–1068.

[70] Chung, C.F. and Fabbri, A.G. (2004). Systematic procedures of landslide hazard mapping for risk assessment using spatial prediction models. In: Landslide hazard and risk. Glade, T., Anderson, M.G. and Crozier, M.J., (Eds.). Wiley, New York, NY, p. 139–174.

[71] Chung, C.F. and Fabbri, A.G. (2008). Predicting landslides for risk analysis - spatial models tested by a cross-validation technique. Geomorphology, 94: 438–452.

[72] Pohar, M., Blas, M. and Turk, S. (2004). Comparison of Logistic Regression and Linear Discriminant Analysis: A Simulation Study. Metodološki Zvezki, 1(1): 143-161.

[73] Guzzetti, F., Malamud, B.D., Turcotte, D.L. and Reichenbach, P. (2002). Power-law correlations of landslide areas in Central Italy. Earth and Planetary Science Letters, 195: 169–183.

[74] Malamud, B.D., Turcotte, D.L., Guzzetti, F. and Reichenbach, P. (2004). Landslide inventories and their statistical properties. Earth Surface Processes and Landforms, 29(6): 687–711.

[75] Guzzetti, F., Galli, M., Reichenbach, P., Ardizzone, F. and Cardinali, M. (2006). Landslide hazard assessment in the Collazzone area, Umbria, Central Italy. Natural Hazards and Earth System Sciences, 6: 115–131.

[76] Lin, L., Lin, Q. and Wang, Y. (2017). Landslide susceptibility mapping on a global scale using the method of logistic regression. Nat. Hazards Earth Syst. Sci., 17: 1411–1424.

[77] Guzzetti, F., Mondini, A.C., Cardinali, M., Fiorucci, F., Santangelo, M. and Chang, K.T. (2012). Landslide inventory maps: New tools for an old problem. Earth-Science Review, 112: 42–66.

[78] Corominas, J., Copons, R., Manuel, J., Vilaplana, A., Altimir, J. and Amigó, J. (2003). Integrated landslide susceptibility analysis and hazard assessment in the principality of Andorra. Natural Hazards, 30: 421–435.

[79] Talaei, R., (2012). Determination and assessment of landslide hazard index in the Hashtjin area (northwestern region of Iran). Bulletin of the Moscow State Regional University, Natural Sciences Series, 1: 69-74.

[80] Turner, A.K. and Schuster, R.L. (1996) Landslides. Investigation and mitigation, Special Report 247, Transportation Research Board. National Academic, Washington, USA, pp. 1-673.

[81] Prabu, S. and Ramakrishnan, S.S. (2009). Combined use of socio economic analysis, remote sensing and GIS data for landslide hazard mapping using ANN. Journal of the Indian Society of Remote Sensing, 37(3): 409–421.

[82] Chen, J., Zeng, Z., Jiang, P. and Tang H. (2015). Deformation prediction of landslide based on functional network. Neurocomputing, 149: 151–157.

[83] Zadeh, L.A. (1965). Fuzzy sets. Information and Control, 8: 338-353.

[84] Chung, C.F. and Fabbri, A.G. (2001). Prediction models for landslide hazard using a fuzzy set approach. In: Geomorphology and Environmental Impact Assessment. Marchetti, M. and Rivas, V., (Eds.). Balkema, Rotterdam, p. 31–47.

[85] Choi, S.W., Moon, W.M. and Choi, S.G. (2000). Fuzzy logic fusion of W-Mo exploration data from Seobyeog-ri, Korea. Geosciences journal, 4(2): 43-52.

[86] Shahabi, H., Khezri, S., Ahmad, B.B. and Allahvirdiasl, H. (2012). Application of satellite and fuzzy set theory in landslide hazard mapping in central Zab basin. IOSR Journal of Applied Physics (IOSRJAP), 1(4): 17-24.

[87] Yalcin, A. (2007). The effects of clay on landslides: A case study. Applied Clay Science, 38: 77-85.

[88] Muntohar, A.S., Hashim, R. (2003). Swelling behavior of Engineered clay soil. The second International Conference on Advances in Soft Soil Engineering and Technology, 2-4 July 2003, Putra Jaya, Malaysia: 865-871.

[89] Talaei, R., Peyrowan, H., Jafari ardekani, A., Beyrami, B. and Ghayomian J. (2013). Classification and determination of erodibility indices of Ardabil Province marls. Soil Conservation and Watershed Management Institute, Agricultural Research, Education and Extension Organization (AREEO), Final Report of research plan, 113 pages (in Persian).

[90] Talaei, R., (2014). Landslide susceptibility zonation mapping using logistic regression and its validation in Hashtchin Region, northwest of Iran. Journal of the Geological Society of India, 84(1): 68-86.

[91] Mugagga, F., Kakembo, V. and Buyinza, M. (2012). A characterisation of the physical properties of soil and the implications for landslide occurrence on the slopes of Mount Elgon, Eastern Uganda. Nat Hazards, 60(3):1113-

1131.

[92] Baynes, F.J. (2008). Anticipating problem soils on linear projects. Conference proceedings on problem soils in South Africa, Midrand, 3-4 November 2008:9-21.

[93] Janalizadeh, A., Ramazanpour, M. (2007). Investigation on improvement of clay soils of Mazandaran province. Civil Engineering Departement, Faculty of Engineering, Tabriz University, 3rd National Congress on Civil Engineering, 1-3, 8 pages (in Persian).

[94] Zung, A.B., Sorensen, C.J. and Winthers, E. (2009). Landslide soils and Geomorphology in Bridger/Teton Forest Northwest Wyoming. Phys Geogr, 30(6): 501–516.

[95] Talayi, R., Shariat Jafari, M. (2008). Study on effective factors causing landslide in the southwest of Khalkhal by using crosstables and chi-square method. Iranian Journal of Engineering Geology, 1(2): 43-62.

[96] Davies, R.G, Clark, G.C., Hamzepour, B. and Jones, C.R. (1975). Explanatory Text of the Bandar-e-Pahlavi quadrangle map, 1:250000. Geological Survey of IRAN, No. D3. 203 pages.

[97] Cardoso, R., Alonso, E.E. (2009). Degradation of compacted marls, A microstructural investigation. Soils and Foundations, 49(3): 315-328.

[98] Bates, R.L., Jackson, J.A. (1980). Glossary of Geology. 2nd edition, American Geological Institute, Falls Church, Virginia, 751 pages.

[99] Talaei, R., Samadov, S. (2012). Landslides characteristics and classifications in Hashtjin area (northwest of - IRAN). Вестник , Bulletin of the Moscow State Regional University, Series, Natural Sciences, 2: 90-94.

[100] Pars Karst Water, (P.K.W.). (2011). Hydrology and water balance study, Karstic water resources and hard formation studies in Khalkhal area. Ardabil regional water company, Iran water resource Management Company. Department of Energy. Research and Exploration Co., Pars Karst Water (P.K.W.), Final report, vol. 4, 152p.

[101] Dragićević, S., Lai, T. and Balram, S. (2015). GIS-based multicriteria evaluation with multiscale analysis to characterize urban landslide susceptibility in data-scarce environments. Habitat International, 45: 114-125.

[102] Mancini, F., Ceppi, C., Ritrovato, G. (2010). GIS and statistical analysis for landslide susceptibility mapping in the Daunia area, Italy. Nat. Hazards Earth Syst. Sci., 10, 1851–1864.

[103] Duman, T.Y., Can, T., Gokceoglu, C., Nefeslioglu, H.A. and Sonmez, H. (2006). Application of logistic regression for landslide susceptibility zoning of Cekmece Area, Istanbul, Turkey. Environmental Geology, 51: 241–256.

[104] Dai, F.C., Lee, C.F. and Wang, S.J. (1999). Analysis of rainstorm-induced slide-debris flows on natural terrain of Lantau Island, Hong Kong. Engineering Geology, 51: 279–290.

[105] Polykretis, C., Ferentinou, M. and Chalkias, C. (2015). A comparative study of landslide susceptibility mapping using landslide susceptibility index and artificial neural networks in the Krios River and Krathis River catchments (northern Peloponnesus, Greece). Bull Eng Geol Environ, 74: 27–45.

[106] Lee, J.H., Sameen, M.I., Pradhan, B. and Park, H.J. (2018). Modeling landslide susceptibility in data-scarce environments using optimized data mining and statistical methods. Geomorphology, 303: 284-298.

[107] Zhu, A.X., Wang, R., Qiao, J., Qin, C.Z., Chen, Y., Liu, J., Du, F., Lin, Y. and Zhu, T. (2014). An expert knowledge-based approach to landslide susceptibility mapping using GIS and fuzzy logic. Geomorphology, 214: 128–138.

[108] Leonardi, G., Palamara, R. and Cirianni, F. (2016). Landslide susceptibility mapping using a Fuzzy approach. Procedia Engineering, 161: 380 – 387

[109] Castellanos Abella, E.A. and van Westen, C.J. (2007). Generation of a landslide risk index map for Cuba using spatial multi-criteria evaluation. Landslides, 4: 311–325.

[110] Hoseinpour M.A., Delavar, M. and Chehreghan, A. (2016). Uncertainty in landslide occurrence prediction using Dempster–Shafer theory. Model. Earth Syst. Environ, 2:188, 10 pages.

[111] Glade, T., Crozier, M.J. (2005). A review of scale dependency in landslide hazard and risk analysis. In: Glade, T., Anderson, M.G. and Crozier, M.J. (eds.), Landslide Hazard and Risk.Wiley, Chichester, 75–138.

Please cite this article using:

R. Talaei, A combined model for landslide susceptibility, hazard and risk assessment, *AUT J. Civil Eng.*, 2(1) (2018) 11-28.

DOI: 10.22060/ajce.2018.14235.5465